An Efficient Flux-Lumped Discontinuous Galerkin Scheme for the 3D Maxwell Equations on Nonconforming Cartesian Grids

Matthieu Patrizio, Bruno Fornet, Vincent Mouysset, Xavier Ferrières

An Efficient Flux-Lumped Discontinuous Galerkin Scheme for the 3D Maxwell Equations on Nonconforming Cartesian Grids

Matthieu Patrizio[1,*], **Bruno Fornet**[1], **Vincent Mouysset**[2], **Xavier Ferrieres**[2]

[1]NUCLETUDES, 3 avenue du Hoggar -Les Ulis -CS 70117- 91978 Courtabœuf Cedex, France

[2]Onera, The French Aerospace Lab, F-31055, Toulouse, France

[*]Email: matthieu.patrizio@gmail.com

Abstract

The Discontinuous Galerkin in Time Domain Method (DGTD) is one of the most promising methods to simulate multiscale phenomena. It combines high order precision (p) with flexible geometries (h) resulting in inhomogeneous hp-approximation spaces. In a cartesian framework we show that some parts of the numerical scheme, namely heterogeneous flux terms, can lead to an outburst of computational cost on nonconforming meshes. A new scheme devoid of this bottleneck and proved to be stable is presented along with numerical results.

Keywords: Discontinuous Galerkin, nonconforming approximation, computational cost

1 Introduction

DG methods build an approximate solution which is piecewise polynomial (p) over the mesh (h). It shows various attractive properties, especially flexibility to multiscale geometries, allowing high precision modelling. However, DGTD solvers have performance bottlenecks which limit its use for industrial purpose, compared to Finite Difference in Time Domain for instance.

One can notice that, in a hp-conforming context, increasing correlatively the approximation order and the mesh size is a powerful strategy to reduce numerical cost. However, in complex geometries, the presence of low-scale inner elements can constrain the mesh, leading to hp-nonconforming configurations (Fig. 1). As shown in the sequel, the latter create extra computational costs, due to nonconforming fluxes, which can invalidate the interest of $hp-$expansion strategies.

We present here a new numerically efficient DGTD scheme based on lumped fluxes for nonconforming cartesian grids. A stability result is provided, as well as a numerical example on electromagnetic wave propagation.

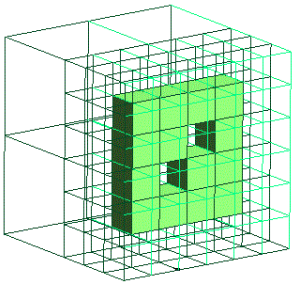

Figure 1: *Usual $h-$nonconforming mesh. The front part is refined to fit with a drilled dielectric plate, the back one is relaxed.*

2 DG Scheme and Performance Issues

We consider 3D time-dependent Maxwell's equations on a cavity Ω, with metallic boundary conditions on $\partial\Omega$:

$$\begin{aligned} \partial_t U + A(\partial)U = 0 \quad &\text{in} \quad (0,T)\times\Omega, \\ B(n_b)U = 0 \quad &\text{in} \quad (0,T)\times\partial\Omega, \\ U(0,\cdot) = U_0 \quad &\text{in} \quad \Omega, \end{aligned}$$

where $U=(E,H)^T$ is the electromagnetic field, $A(\partial):(E,H)\mapsto(-\nabla\wedge H,\nabla\wedge E)^T$ the Maxwell differential operator, $B(n_b):(E,H)^T\mapsto(0,-n_b\wedge E)^T$ the boundary condition operator, n_b the unit outward normal, and U_0 the initial data. This problem is well-posed in $\mathfrak{U}=\mathcal{C}^0\big((0,T);H_{curl}(\Omega)^2\big)$. Denoting by T_h the mesh, F_{int} and F_{bound} the sets of interior and boundary faces, and $\mathfrak{U}_{hp}$ the approximation space of $\mathfrak{U}$, DG usual variational formulation holds:

$$\begin{aligned} &\textit{For all } t\in(0,T),\ \textit{find } \big(u(t,\cdot),\phi\big)\in\big(\mathfrak{U}_{hp}\big)^2,\ \textit{such as:} \\ &\sum_{K\in T_h}\Bigg[\underbrace{\langle\partial_t u,\phi\rangle_K}_{\text{mass}}+\underbrace{\langle A(\partial)u,\phi\rangle_K}_{\text{stiffness}}+\sum_{\substack{f\subset\partial K\\ f\in F_{bound}}}\underbrace{\langle B(n_b)u,\phi\rangle_f}_{\text{bound. flux}}+ \\ &\sum_{\substack{f\subset\partial K\\ f\in F_{int}}}\underbrace{\big\langle[\![M(n_f)u]\!]_f,\phi^-\big\rangle_f-\big\langle[\![M(-n_f)u]\!]_f,\phi^+\big\rangle_f}_{\text{int. fluxes}}\Bigg]=0, \end{aligned} \tag{1}$$

where $M(n_f)=A(n_f)-\beta N(n_f)$, is the flux matrix accross a given face f with arbitrary unit normal n_f, $A(n_f)$ and $N(n_f)$ the centered and upwind parts, and $\beta\in[0,1]$ an upwinding parameter. $\phi^{\pm}$ stands for the trace of ϕ on both sides of f, $[\![\cdot]\!]$ is the jump accross f and $\langle\cdot,\cdot\rangle_K$ is the usual $\mathcal{L}^2(K)^6$ scalar product. Discretization of (1) is led using Line-Based method [1]

in space and Leapfrog integration in time. This DGTD scheme uses Gauss-Lobatto basis functions with a lumping method to compute mass, stiffness and conforming flux terms. Table 1 shows the numerical costs for three different configurations giving the same level of accuracy:

Config.	CPU-time (w.r.t. Q^1)	Dofs ($\times 10^3$)
Q^1	1.0	93
Q^2	0.13	10
Q^1/Q^2	52	47

Table 1: *Comput. costs on* 12^3 *mesh with* Q^1 *functions,* 4^3 *with* Q^2*, and related* Q^1/Q^2 *hybrid config.*

One can notice that CPU-time on hybrid configuration (t) is about 50 times more important than on the Q^1 refined mesh (t_{ref}), while expected to be $\frac{t_{ref}}{2} \leq t \leq t_{ref}$. A cost tracking led on this computation revealed this is due to nonconforming fluxes involved in Q^1/Q^2 coupling, computed with standard exact surface quadratures. Thus, a new handling of these terms is developped, so-called flux-lumping, to recover a satisfactory level of performance.

3 The Flux-Lumped (FL) DG Approach

The idea is to consider the flux term across a nonconforming surface S_{nc} as one global quantity, instead of several local fluxes. Each interior flux in (1) is splitted into 4 terms, corresponding to homogeneous $(\pm.\pm)$ and heterogeneous $(\pm.\mp)$ centered and upwind parts. Homogeneous terms are treated as before, nonconforming heterogeneous ones can be lumped but have to be rebalanced to ensure scheme stability. Given $\Gamma^{\pm}$, the trace spaces of u on $S_{nc}^{\pm}$, we define two reconstruction operators $\Pi_{S_{nc}}^{\pm} : \Gamma^{\mp} \longrightarrow \Gamma^{\pm}$, by:

$$\Pi_{S_{nc}}^{\pm}\left(A^{\mp}u^{\mp}\right) = \sum_{j=1}^{N_{dof}^{\pm}} \widehat{\pi}_j^{\pm}(u^{\mp})\mathscr{P}_{f(j)}\left(\widehat{A}^{\pm}\widehat{L}_j^{\pm}\right)\mathbf{1}_{f(j)},$$

where $A^{\pm} = A(\mp n)$, $\widehat{\pi}_j^{\pm}(u^{\mp}) \in \mathbb{R}$, $f(j)$ is the sub-face containing dof j, $\mathscr{P}_{f(j)}$ is the $(H_{curl})^2$ surface-conforming transformation, $\widehat{A}$ and $(\widehat{L}_j)_j$ are the matrix A and basis functions expressed in the reference element $[-1,1]^3$. Finally, the heterogeneous nonconforming flux-lumping holds:

$$\langle \Pi_{S_{nc}}^{\pm}(A^{\pm}u^{\mp}), \phi^{\pm}\rangle_{S_{nc}}^{\pm} = \sum_{j=1}^{N_{quad}^{\pm}} \omega_j^{\pm}\Pi_{S_{nc}}^{\pm}(A^{\pm}u^{\mp})(\sigma_j^{\pm}).\phi^{\pm}(\sigma_j^{\pm}), \tag{2}$$

where $(\omega_j^{\pm}, \sigma_j^{\pm})_j$ are surface quadrature weights and points, fulfilling the following conditions:

- **(C1) Consistency:** $\forall u^{\pm} \in \Gamma^{\pm}$,

$$\langle \Pi_{S_{nc}}^{-}(A^{+}u^{+}), u^{-}\rangle_{S_{nc}}^{-} = \langle \Pi_{S_{nc}}^{+}(A^{-}u^{-}), u^{+}\rangle_{S_{nc}}^{+},$$

and either

$$\langle A^{-}u^{-}, A^{-}u^{-}\rangle_{S_{nc}}^{-} = \langle \Pi_{S_{nc}}^{+}(A^{-}u^{-}), \Pi_{S_{nc}}^{+}(A^{-}u^{-})\rangle_{S_{nc}}^{+},$$

or the same identity switching signs $+$ and $-$.

- **(C2) Positivity:**

$$\forall u^{\pm} \in \Gamma^{\pm},\ \langle A^{\pm}u^{\pm}, A^{\pm}u^{\pm}\rangle_{S_{nc/c}}^{\pm} \geq 0\,.$$

We thus proved the following stability result:

Theorem 1 *Given* $u \in \mathfrak{U}_{hp}$*, if* $(\omega_j^{\pm}, \sigma_j^{\pm})_j$ *in* (2) *are satisfying (C1) and (C2), then the semi-discrete energy associated to the Gauss-Lobatto Flux-Lumped DG approach decreases:* $\forall t \in (0,T)$,

$$\frac{de}{dt}(t) \leq 0, \quad \textit{with}\ \ e(t) = \frac{1}{2}\sum_{K\in T_h}\langle u,u\rangle_K\,.$$

4 Numerical Example

Computing propagation of 1-modes using flux-lumping approach on the hybrid configuration, the expected numerical efficiency is reached, see Fig. 2 and Table 2.

Config.	CPU-time (w.r.t. Q^1)	Dofs ($\times 10^3$)
FL Q^1/Q^2	0.86	47

Table 2: *Computational costs with FLDGTD scheme on the hybrid configuration (same accuracy).*

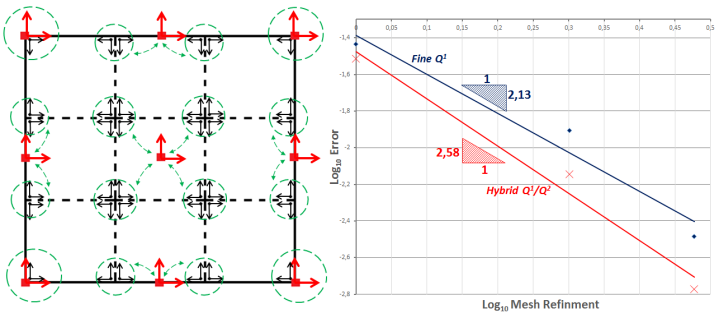

Figure 2: Left: Nonconforming surfaces and reconstruction operators used in the example. Right: $\mathcal{L}^2$*-space/*$\mathcal{L}^1$*-time error w.r.t mesh isotropic refinment factor.*

References

[1] P. Persson, *High-Order Navier-Stokes Simulations using a Sparse Line-Based Discontinuous Galerkin Method*, AIAA 2012-0456 (2012).

Acknowledgements This work is financially supported by The French Ministry of Defence-DGA.